Clinical Investigative Study

Correlation between Cognitive Deficits and Glucose Hypometabolism in Mild Cognitive Impairment

Hiroko Nishi, MD, Nobukatsu Sawamoto, MD, PhD, Chihiro Namiki, MD, Hidefumi Yoshida, MD, Dinh Ha Duy Thuy, MD, PhD, Koichi Ishizu, MD, PhD, Kazuo Hashikawa, MD, PhD, Hidenao Fukuyama, MD, PhD

From the Human Brain Research Center, Kyoto University Graduate School of Medicine, Shogoin, Sakyo-Ku, Kyoto, Japan (HN, NS, CN, HY, DHDT, KH, HF); Department of Psychiatry, Kyoto University Graduate School of Medicine, Shogoin, Sakyo-Ku, Kyoto, Japan (CN); Department of Nuclear Medicine and Diagnostic Imaging, Kyoto University Graduate School of Medicine, Shogoin, Sakyo-Ku, Kyoto, Japan (KI).

ABSTRACT

BACKGROUND

In patients with mild cognitive impairment (MCI), poor performances on delayed recall and executive function are risk factors of progression to dementia. The aim of the present study was to clarify neural correlates of these neuropsychological deficits.

METHODS

Thirty patients with amnestic MCI and 15 control subjects underwent neuropsychological tests including three-word delayed recall, visual delayed recall of Rey complex figure (RCF), and two-relational reasoning of Raven's colored progressive matrices (RCPM) with a ^{18}F-fluorodeoxyglucose (FDG)-position emission tomography (PET) measurement of resting state. We evaluated a relationship between performance of neuropsychological tests and regional cerebral glucose metabolism using voxel-based analysis.

RESULTS

Poor performance in three-word delayed recall was related to glucose hypometabolism in the right medial temporal, right prefrontal, and left superior parietal cortices. The deficit in visual delayed recall of RCF correlated positively with hypometabolism in the bilateral posterior cingulate. The impairment in two-relational reasoning was associated with hypometabolism in the right prefrontal cortex.

CONCLUSIONS

The present findings suggest that hypometabolism in the right medial temporal cortex, right prefrontal cortex, left superior parietal cortex, and bilateral posterior cingulate reflects impairments in delayed recall while hypometabolism in the right prefrontal cortex mirrors deficits in executive function in MCI.

Keywords: Dementia, psychology, positron emission tomography, mild cognitive impairment, episodic memory, executive function.

Acceptance: Received August 17, 2008, and in revised form August 17, 2008. Accepted for publication September 15, 2008.

Correspondence: Address correspondence to Nobukatsu Sawamoto, MD, PhD, Human Brain Research Center, Kyoto University Graduate School of Medicine, 54 Kawahara-machi, Shogoin, Sakyo-Ku, Kyoto 606-8507, Japan. E-mail: sawa@kuhp.kyoto-u.ac.jp.

Conflict of Interest: None.

J Neuroimaging 2008;XX:1-8.
DOI: 10.1111/j.1552-6569.2008.00328.x

Introduction

Mild cognitive impairment (MCI) has been postulated as a prodromal state of dementia. More than half of patients with MCI are estimated to progress to dementia within 5 years.[1] However, some seem to remain stable or even return to normal over time. One of the risk factors for progression to dementia in patients with MCI is poor performance on delayed recall and executive function.[2,3] Although it is tempting to presume neuroanatomical substrates causing this poor performance based on the findings of healthy subjects, the substrates underlying the cognitive process may be partly reorganized in the diseased brain of patients with MCI possibly due to neurodegenerative changes or functional compensation.

Neuronal substrates underlying delayed recall and executive function have been largely unexplored in MCI whereas those have been well studied in Alzheimer's disease (AD). It might be possible to speculate that patients with MCI share similar but milder changes, at least in part, with those in AD. Neuroimaging studies in MCI suggest that impairments in verbal episodic memory are associated with glucose hypometabolism in the right medial temporal cortex and bilateral posterior cingulate, and volumetric decrease in the bilateral medial temporal cortex.[4,5] Meanwhile, series of studies in AD have already demonstrated that the impairments are related to hypometabolism in the bilateral medial temporal cortex, posterior cingulate, and prefrontal cortex[6-11] and atrophy in the left medial temporal cortex and bilateral inferior frontal gyrus.[12-16]

As for deficits in visual episodic memory in MCI, neural correlates are still unclear while many studies have shown that the deficits in AD are linked to hypometabolism in bilateral temporal and parietal cortex.[6,9,17,18] Neural substrates underlying executive dysfunction in MCI also remain unknown whereas studies have revealed that the dysfunction of AD reflects hypometablism in bilateral frontal and tempo-parietal cortex.[19,20]

Table 1. Demographic and Clinical Characteristics of Patients with MCI and Controls

	MCI	Controls
Number	30	15
Age (years)	69.8 ± 7.3	70.9 ± 4.2
Gender (female/male)	22/8	9/6
Education (years)	11.3 ± 2.8	12.0 ± 2.2
WMS-R logical memory	5.1 ± 3.6* (0-11)	20.7 ± 6.3 (12-33)
MMSE total score	26.5 ± 2.1* (24-30)	29.1 ± 1.6 (26-30)
RCF copy	33.3 ± 2.6 (28-36)	34.3 ± 2.8 (31-36)
FAB	15.3 ± 2.3 (9-18)	15.4 ± 1.2 (14-18)

Numbers correspond to mean ± standard deviation (ranges) in this and related tables.
WMS-R = Wechsler Memory Scale-revised; MMSE = Mini-Mental State Examination; RCF = Rey complex figure; FAB = Frontal Assessment Battery.
*Significant difference at $P < .05$.

The aim of the present study was to investigate neuroanatomical substrates underlying the poor performance of verbal and visual delayed recall and executive function specifically in patients with MCI. For this purpose, 30 patients with MCI and 15 control subjects underwent neuropsychological tests including three-word delayed recall, visual delayed recall of Rey complex figure (RCF), and two-relational reasoning of Raven's colored progressive matrices (RCPM) together with a ^{18}F-fluorodeoxyglucose (FDG)-position emission tomography (PET) measurement of resting state. We investigated neural correlates of neuropsychological deficits by examining correlation between scores of neuropsychological tests and FDG-PET uptake. Since it seems possible to expect that patients with MCI share similar neural correlates, at least in part, with those in healthy controls and AD patients, we expected that deficit in three-word delayed recall is associated with glucose hypometabolism in the bilateral medial temporal cortex, prefrontal, and parieto-occipital areas based on neuroimaging studies on verbal retrieval.[6-11,21-24] We predicted that poor performance of visual delayed recall is associated with hypometabolism in the bilateral medial temporal, prefrontal cortices, and parieto-occipital areas based on studies on visual retrieval.[6,9,21,24-27] We also expected the significant correlation between the poor performance of two-relational reasoning and hypometabolism in the bilateral prefrontal cortex following studies on executive function including relational reasoning task.[28-30]

Methods

Subjects

Subjects comprised 30 amnesic MCI patients (Table 1). They were diagnosed according to the criteria, which generally follow previous MCI studies[31-33]: (1) memory complaints by patient or informant; (2) objective memory impairment, presenting as a logical memory (immediate recall) score on the Wechsler Memory Scale-revised (WMS-R) < 1.5 standard deviations (SDs) below the mean for age-matched controls[34]; (3) Clinical Dementia Rating (CDR) score of .5[35]; (4) preserved activities of daily living (ADL)[36,37]; (5) preserved general cognitive function, Mini-Mental State Examination (MMSE) score ≥24[38]; and (6) not meeting National Institute of Neurological and Communication disorders and Stroke/AD and Related Disorders Association (NINCDS-ADRDA) criteria for probable AD.[39] None of the patients have received any medication known to affect brain metabolism including anticholinergic therapies. Patients were recruited prospectively at the outpatient clinic of the Dementia Unit at Kyoto University Hospital between March 2004 and January 2006.

Fifteen healthy controls matched for age and level of education were also registered, and received the same neuropsychological tests. Inclusion criteria for controls were as follows: (1) physically and mentally healthy and not experiencing or exhibiting any cognitive impairment; (2) CDR score of 0. Controls were recruited between June 2004 and December 2005.

MCI patients and healthy controls were excluded based on: (1) complications of other medical illnesses possibly causing cognitive impairment, such as thyroid disease, vitamin deficiencies, and malignant disease; (2) mental disease, substance abuse, or significant neurological antecedents (eg, stroke, brain hemorrhage, trauma, tumors, epilepsy, vascular dementia, other dementing illnesses, and inflammatory disease); or (3) evidence of brain infarctions or extensive white matter lesions on magnetic resonance imaging (MRI) in T1- and T2-weighted and fluid attenuated inversion recovery (FLAIR) images.

All subjects were right-handed. All MCI patients and controls were interviewed and received examinations by neurologists and psychiatrists. They were also examined with routine laboratory tests. All participants and/or their responsible guardians provided written informed consent in accordance with the approval by the Ethical Committee of Kyoto University Graduate School of Medicine.

Neuropsychological Assessments

All subjects received neuropsychological tests of verbal and visual delayed recall, and executive function. Verbal delayed recall was evaluated using three-word delayed recall from MMSE since this was sensitive to dementia[40,41] and can be administered in several minutes. To evaluate visual delayed recall, 3-min delayed recall of RCF was conducted after confirming that the performance of RCF copy was preserved (Table 1).[41] We measured executive function using eight two-relational reasoning problems in RCPM.[42-44] This test has been used to assess executive function,[45,46] particularly nonverbal abstract reasoning, which requires simultaneous integration of multiple dimensions of information.[44,47,48] It is easy to undertake even at an outpatient clinic without complicated instructions, although additional testing may be required to confirm that the patients have preserved visuospatial function. The Frontal Assessment Battery (FAB) was evaluated to confirm that patients did not suffer from general frontal dysfunction (Table 1).[49]

Differences in demographic and neuropsychological data between groups were evaluated using SPSS software (SPSS Inc., Chicago, IL). Nonparametric Mann-Whitney U-tests were used

for comparisons between groups. For these analyses, values of $P < .05$ (two-tailed) were considered indicative of statistical significance.

FDG-PET Data Acquisition

PET data were acquired using a GE Advance system (GE/Yokogawa, Tokyo, Japan). The scanner acquired 35 slice images with a slice thickness of 4.25 mm in 2-dimensional mode. Axial dimension and pixel size of the reconstructed images were 128 and 1.95 mm, respectively. All subjects were fasted for ≥4 hours before scanning. To obtain transaxial images, subjects were positioned with the canthomeatal line parallel to the detector ring and the head was kept in a fixed position using a head holder. At 40 min after bolus injection of 370 MBq of [^{18}F]-FDG, a 15-min measurement of FDG uptake was started in the resting condition, with eyes closed, in a quiet and dark environment. Data were corrected for effects of radiation attenuation using a 5-min transmission scan with ^{68}Ge. Images were reconstructed using an ordered subset expectation maximization algorithm.

Data Analysis

FDG-PET images were analyzed using SPM2 software (Wellcome Department of Cognitive Neurology, London, UK) implemented in MATLAB (MathWorks Inc., Natick, MA). Images were spatially transformed to a standard stereotaxic space using the Montreal Neurological Institute (MNI) PET template. An isotropic Gaussian filter was used to smooth the spatially normalized images with a full width at half maximum (FWHM) of 12 mm. Following previous studies,[4,6,7,11,50,51] we normalized individual global counts by proportional scaling. We then obtained relative regional cerebral glucose metabolism images with a mean value of 5.0 mg/100 mL/min, which were subjected to statistical analysis using a general linear model. For all statistical analyses, those voxels with values >80% of the mean for the whole brain were selected.

First, differences in brain glucose uptake between patients with MCI and healthy controls were evaluated. We report statistical peaks that reached $P < .05$ corrected for multiple comparisons (cluster level). We also report statistical peaks that reached $P < .001$ uncorrected with more than seven contiguous voxels in the bilateral medial temporal cortex and posterior cingulate since hypometabolism in those areas has been already shown in previous studies of MCI.[4,52-55] Second, multiple linear regression analysis put three neuropsychological tests (three-word delayed recall on MMSE, 3-min delayed recall of RCF, and two-relational reasoning in RCPM) together was assessed in the MCI group, in consideration of possible intercorrelation among performances of these tests. We also conducted simple linear correlation analysis to confirm the relationships between the uptake and performance of three tests separately. Age was treated as covariates of no interest for both multiple linear regression and simple linear correlation analyses. For these analyses, statistical peaks that reached $P < .05$ corrected for multiple comparisons (cluster level) were evaluated as significant. Predicted statistical peaks that reached $P < .001$ uncorrected with more than seven contiguous voxels were also reported.

Table 2. Performance of Neuropsychological Tests

	MCI	Controls
Three-word delayed recall	1.8 ± 1.1* (0-3)	2.9 ± .3 (2-3)
RCF delayed recall	8.4 ± 8.5* (0-28)	15.4 ± 6.7 (7-25)
RCPM two-relational reasoning	3.6 ± 2.1* (0-8)	5.9 ± 1.3 (5-8)

RCF = Rey complex figure; RCPM = Raven's colored progressive matrices.
*Significant difference at $P < .05$.

Since data points of three-word delayed recall seem to be not enough for parametric test, relationship between the score and magnitude of glucose uptake was further investigated using nonparametric test. We conducted Spearman's rank correlation between the score and averaged value of glucose uptake in a significant cluster identified in the multiple linear regression analysis.

These correlation analyses were not assessed in healthy controls because of the low variance in neuropsychological data.

Results

Patients with MCI showed performance deficits compared to controls in three-word delayed recall of MMSE and 3-min delayed recall of RCF (Table 2). Patients also showed lower performance on two-relational reasoning in RCPM.

Comparison of FDG-PET data between the groups demonstrated reductions of glucose uptake in the posterior cingulate cortex in patients with MCI (Fig 1).

Multiple linear regression analysis between the score of three-word delayed recall and relative regional glucose uptake showed a significant relationship between performance deficits and lower uptake in the bilateral medial temporal cortex, right prefrontal cortex, and left superior parietal cortex, suggesting that the deficits are linked to hypometabolism in these areas in MCI (Figs 2A and 3A; Table 3). Performance deterioration of visual delayed recall was associated with lower uptake in

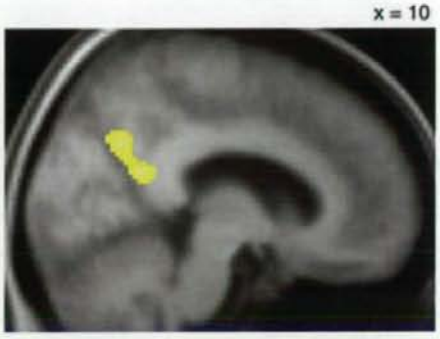

Fig 1. Pattern of reduced brain glucose metabolism in patients with MCI compared to healthy controls. For display purposes in this and related figures, statistical parametric maps are presented at $P<.005$ uncorrected for multiple comparisons on averaged MRI slice images.

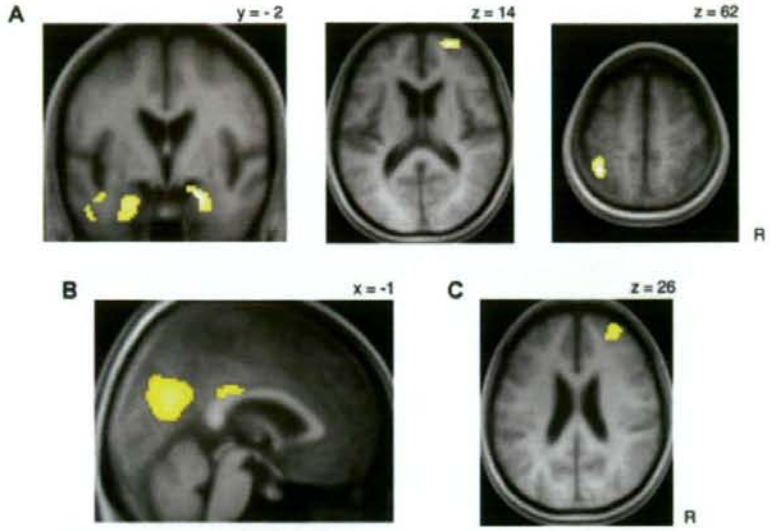

Fig 2. Brain areas exhibiting a positive linear relationship between regional glucose uptake and (A) three-word delayed recall, (B) Rey complex figure (RCF) delayed recall, and (C) Raven's colored progressive matrices (RCPM) two-relational reasoning test. R, subject's right side.

the bilateral posterior cingulate, consistent with an association between impaired performance and metabolic reductions in the brain areas (Figs 2B and 3B; Table 3). The score of two-relational reasoning in RCPM declined as glucose uptake decreased in the right middle frontal gyrus and right superior frontal gyrus, suggesting that the poor performance was related to hypometabolism in those areas (Figs 2C and 3C; Table 3). Simple linear correlation analysis produced generally similar results as those of multiple linear regression analysis. We confirmed that there were linear relationships between deficits of three-word delayed recall and lower uptake in the right medial temporal cortex, right prefrontal cortex, and left superior parietal cortex. We also confirmed linear relationships between deterioration of visual delayed recall and lower uptake in the bilateral posterior cingulate, and impairments in two-relational reasoning task and uptake reduction in the right middle frontal gyrus.

The validity of the multiple linear regression analyses was confirmed since the values of variance inflation factors (VIF) among the three neuropsychological scores were 1.1-1.5 and the scores were not considered to have multicollinearity.

Table 3. Brain Areas Showing Cerebral Glucose Uptake Reduction with Relation to Poor Performance on Neuropsychological Tests in MCI: Multiple Linear Regression Analysis

			Coordinates			
	BA	*k*	*x*	*y*	*z*	*Z* Score
Three-word delayed recall						
R parahippocampal gyrus	28	38	20	−2	−22	3.31*
L parahippocampal gyrus	28	27	−26	4	−30	3.20*
R middle frontal gyrus	10	22	22	58	14	3.20*
L superior parietal cortex	7	21	−38	−52	62	3.35*
RCF delayed recall						
L posterior cingulate	31	566	−10	−62	12	4.92**
R posterior cingulate	31	21	4	−24	30	3.20*
RCPM two-relational reasoning						
R middle frontal gyrus	9	29	28	48	26	3.30*
R middle frontal gyrus	46	27	44	22	14	3.38*
R superior frontal gyrus	8	26	18	14	50	3.37*

k = cluster size; BA = Brodman Area; L = left; R = right.
*$P < .001$ uncorrected for predicted peaks.
**$P < .05$ corrected (cluster level).

With Spearman's rank correlation (two-tailed), we confirmed that performance of three-word delayed recall deteriorate as glucose uptake decrease in the right medial temporal cortex ($r = .58$, $P < .01$), right prefrontal cortex ($r = .59$, $P < .01$), and left superior parietal cortex ($r = .62$, $P < .01$).

Discussion

The present patients with MCI displayed behavioral impairment in three-word delayed recall task, visual delayed recall of RCF, and two-relational reasoning of RCPM compared to healthy controls. Glucose metabolism in patients was reduced in the posterior cingulate. Poor performance on three-word delayed recall was related to glucose hypometabolism in the right medial temporal cortex, right prefrontal cortex, and left superior parietal cortex. These neuropsychological and FDG-PET findings in patients with MCI were consistent with the findings of previous studies.[52,55,56] The present study further demonstrated that deficits of visual delayed recall and reasoning task correlated with metabolic reductions in a network of brain areas in patients with MCI. The deficit in visual delayed recall of RCF was related to glucose hypometabolism in the bilateral posterior cingulate. Patients with MCI showed impairments in two-relational reasoning and this correlated with hypometabolism in the right middle frontal gyrus.

Acknowledging the possible controversial points and limitations of this study is important. First, diagnostic criteria for MCI in the present study required only memory impairment in verbal immediate recall, which is a simple and useful approach as an actual clinical test. Although diagnostic criteria involving memory impairments have been proposed by Petersen et al.,[1] no specific neuropsychological battery has been defined to evaluate this function. Previous studies, therefore, evaluated memory impairments using a variety of psychological batteries for verbal, visual delayed, or immediate recall. Patients in those studies showed generally similar neuropsychological characteristics and FDG-PET findings compared with the present patients.[52,55,56] Concluding that the present patients fall into the concept of MCI proposed by Petersen and are comparable with those in previous studies thus seems reasonable. Second, correction for brain atrophy was not performed, and a partial volume effect caused by brain atrophy could have influenced the present results of reduced metabolism. Several previous studies using voxel-based atrophy correction reported that the degree of brain atrophy was relatively independent from the degree of hypometabolism in patients with AD.[50,57] However, patterns of brain atrophy in AD might differ from those in MCI and the effect of atrophy should be considered as a confounding factor.[58] Third, we used three-word delayed recall of MMSE for the evaluation of verbal memory since this was sensitive to dementia[40,41] and can be administered in several minutes. However, this test only gives a rough estimate of verbal memory using three words and one recall trial. Standard batteries for verbal episodic memory (eg Rey Auditory–verbal learning test and California verbal learning test) have more sufficient number of words and recall trials.[41] The greater variability in scores of the standard batteries probably causes higher sensitivity, leading to wider areas of significant correlation including posterior cingulate in previous FDG-PET studies on AD and MCI.[4,6,11] Since four data points of three-words delayed recall seem to be not enough for parametric analysis, we confirmed the significant relationship between the score and glucose uptake using nonparametric test as well.

We conducted multiple linear regression analysis examining combined effects of three neuropsychological deficits on FDG-PET uptake together. Although multiple linear regression analysis is expected to be superior to identify specific connection between the deficits and regional uptake reduction, this methodology carries an assumption that three deficits are not highly correlated each other. Since this assumption can be a matter of debate, we also conducted simple linear correlation analysis to investigate linear relationships between glucose uptake and performance of three neuropsychological tests separately and the findings were similar to the results of multiple linear regression analysis. We interpret that the findings of the two analyses generally agree and strengthen each other in the present study.

It might be reasonable to predict that regions correlated with performance deterioration of the tasks should be involved in brain areas with reduced metabolism in MCI group. Although the regions for visual delayed recall are indeed involved, the regions for three-word delayed recall and two-relational reasoning task were found outside the areas with significant reduction. One reason for this point might be attributable to relatively preserved performance in some of the MCI patients in three-word delayed recall and two-relational reasoning task (Fig 3). The preserved performance in those patients, presumably associated with preserved metabolism in the correlated brain areas, might make the group difference less than statistically significant level. Another reason might be attributable to methodological issue of data analysis. The present study did not employ absolute cerebral glucose metabolic rate but used relative metabolic rate in which FDG uptake value of each voxel was scaled by global mean of the whole brain. This methodology can be affected by global reduction of metabolism in patients with MCI, resulting in overestimation of metabolic rate and lower sensitivity of regional reduction.[59] It was recommended, therefore, that FDG uptake should be scaled by regional value of preserved metabolism such as cerebellar vermis.[6,20,60] Scaling with cerebellar vermis is likely to be a better estimate of absolute glucose metabolic rate compared to scaling with global mean, although it is still possible that smaller region might make the scaling value unstable. In the present study, we selected rather conservative and lower sensitivity method of scaling with global mean to avoid false positives.

Neuroimaging studies on healthy subjects revealed that verbal episodic memory involves activities in the left or bilateral medial temporal cortex.[21-24,61,62] The present study in patients with MCI showed linear relationship between deficits of episodic verbal memory and lower FDG uptake in the right medial temporal cortex in simple linear correlation and multiple linear regression analyses. It seems possible to expect that patients with MCI show similar changes, at least in part, to those in patients with AD. Indeed, poor performance on verbal episodic memory in probable AD was shown to be associated with hypometabolism in the right medial temporal cortex.[6,7]

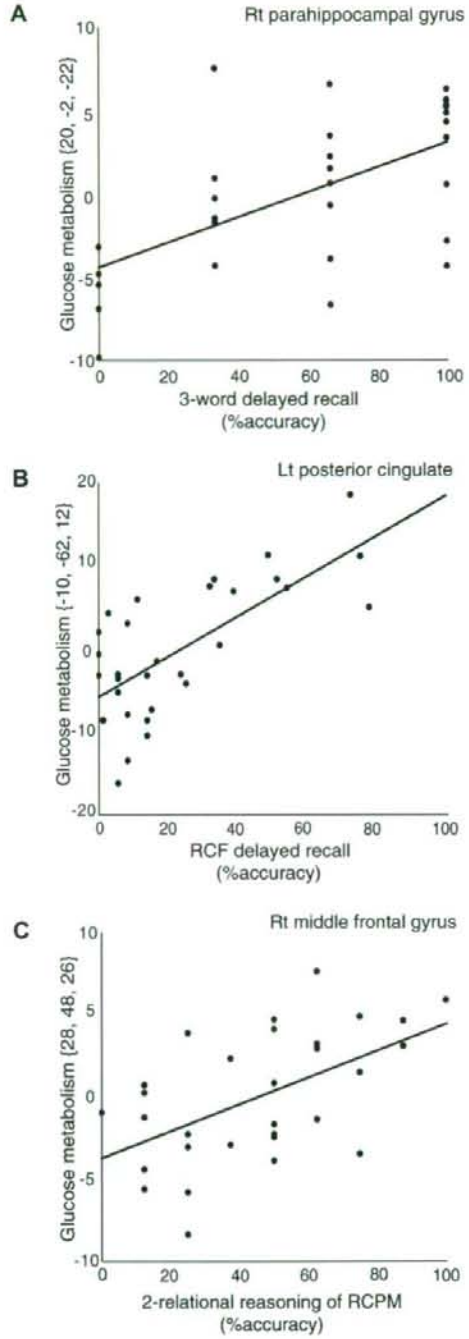

Fig 3. Normalized relative regional glucose metabolism as a function of percentage accuracy in multiple linear regression analyses for (A) three-word delayed recall, (B) Rey complex figure (RCF) delayed recall, and (C) Raven's colored progressive matrices (RCPM) two-relational reasoning test. Each plot corresponds to individual patients with MCI.

The findings might imply that patients with MCI and early-stage AD display increased reliance on the right medial temporal cortex as a compensatory mechanism, and malfunction results in deteriorated performance for verbal episodic memory. A previous study on MCI revealed that encoding deficit of verbal episodic memory correlates with partial volume effect corrected glucose hypometabolism in the right medial temporal cortex whereas retrieval deficit of verbal episodic memory correlated with volume reduction of the bilateral medial temporal cortex.[4] Therefore, the present findings might represent a mix of hypometabolism and atrophy of the right medial temporal cortex reflecting encoding and retrieval deficit in patients with MCI.

The present study also showed that deficits of episodic verbal memory in patients with MCI were related to reduction of glucose uptake in the left superior parietal cortex. The association between the deficits and glucose hypometabolism in the bilateral parietal cortex was reported in patients with AD as well.[6,18] Hypometabolism of the parietal cortex might reflect pathological changes of the area, since a neuropathological study revealed that the area contains the highest amount of neurofibrillary tangles (NFTs) after the temporal lobes in MCI.[63,64]

Episodic memory for visual information is processed in the posterior cingulate cortex in healthy subjects.[26,65] A functional MRI study revealed reduced activation in the posterior cingulate cortex during visual memory recollection in patients with MCI compared to healthy subjects.[66] Lower performance of visual episodic memory has also been shown to correlate with hypometabolism in the posterior cingulate cortex in patients with AD.[6,9] These findings seem to be in line with the present results demonstrating a relationship between deficit in visual delayed recall of RCF and reduction of glucose uptake in the posterior cingulate cortex in patients with MCI. Since pathological changes in the posterior cingulate cortex are relatively mild in MCI, hypometabolism might reflect disconnection to this area from limbic structures suffering severe pathological changes of NFTs in MCI.[64,67-69]

The present patients with MCI showed impaired performance of a relational reasoning task adapted from the Raven's matrices test. It is believed that Raven's matrices test requires series of visual pattern matching and analogical inference reflecting intelligence or generalized cognitive skill.[43,70] In addition, the relational reasoning task seems to involve cognitive process associated with executive function, such as planning, dual task coordination, response selection, and working memory.[19,28] Therefore, the present findings seem to correspond with recent neuropsychological studies proposing that most patients with MCI have not only memory impairment but also additional deficits in multiple cognitive domains including executive function.[56,71-73] Our study also showed that the performance deficits of the relational reasoning task correlated with reduced glucose uptake in the right middle frontal gyrus. The FDG findings are supported by a neuroimaging study of healthy subjects showing significant activation in the right middle frontal gyrus during relational reasoning task.[28] Since the right middle frontal gyrus is associated with response selection across different stimulus materials, this aspect of the task might

be related to the performance deficits and reduced metabolism in the area observed in patients with MCI.[74] Hypometabolism in the prefrontal region might reflect not only increases in NFTs and Senile plaques of the area but also disconnection of links from parietal areas affected with significant neuropathological changes in MCI.[20,64,75-77]

We wish to thank Drs. Tomoko Okina, Norio Suzuki, Yasuhiro Nagahama, Minoru Matsuda, and Naoki Fujimoto for their kind support. This research was partly funded by a Grant-in-Aid for Scientific Research on Priority Areas System study on higher-order brain functions (18020014) from the Ministry of Education, Culture, Sports, Science, and Technology of Japan.

References

1. Petersen RC, Smith GE, Waring SC, et al. Mild cognitive impairment: clinical characterization and outcome. *Arch Neurol* 1999;56:303-308.
2. Chen P, Ratcliff G, Belle SH, et al. Cognitive tests that best discriminate between presymptomatic AD and those who remain nondemented. *Neurology* 2000;55:1847-1853.
3. Jacobs DM, Sano M, Dooneief G, et al. Neuropsychological detection and characterization of preclinical Alzheimer's disease. *Neurology* 1995;45:957-962.
4. Chetelat G, Desgranges B, de la Sayette V, et al. Dissociating atrophy and hypometabolism impact on episodic memory in mild cognitive impairment. *Brain* 2003;126:1955-1967.
5. Convit A, De Leon MJ, Tarshish C, et al. Specific hippocampal volume reductions in individuals at risk for Alzheimer's disease. *Neurobiol Aging* 1997;18:131-138.
6. Desgranges B, Baron JC, de la Sayette V, et al. The neural substrates of memory systems impairment in Alzheimer's disease. A PET study of resting brain glucose utilization. *Brain* 1998;121(Pt 4):611-631.
7. Desgranges B, Baron JC, Lalevee C, et al. The neural substrates of episodic memory impairment in Alzheimer's disease as revealed by FDG-PET: relationship to degree of deterioration. *Brain* 2002;125:1116-1124.
8. Eustache F, Desgranges B, Giffard B, et al. Entorhinal cortex disruption causes memory deficit in early Alzheimer's disease as shown by PET. *Neuroreport* 2001;12:683-685.
9. Perani D, Bressi S, Cappa SF, et al. Evidence of multiple memory systems in the human brain. A [18F]FDG PET metabolic study. *Brain* 1993;116(Pt 4):903-919.
10. Slansky I, Herholz K, Pietrzyk U, et al. Cognitive impairment in Alzheimer's disease correlates with ventricular width and atrophy-corrected cortical glucose metabolism. *Neuroradiology* 1995;37:270-277.
11. Teipel SJ, Willoch F, Ishii K, et al. Resting state glucose utilization and the CERAD cognitive battery in patients with Alzheimer's disease. *Neurobiol Aging* 2006;27:681-690.
12. Deweer B, Lehericy S, Pillon B, et al. Memory disorders in probable Alzheimer's disease: the role of hippocampal atrophy as shown with MRI. *J Neurol Neurosurg Psychiatr* 1995;58:590-597.
13. Duarte A, Hayasaka S, Du A, et al. Volumetric correlates of memory and executive function in normal elderly, mild cognitive impairment and Alzheimer's disease. *Neurosci Lett* 2006;406:60-65.
14. Laakso MP, Soininen H, Partanen K, et al. Volumes of hippocampus, amygdala and frontal lobes in the MRI-based diagnosis of early Alzheimer's disease: correlation with memory functions. *J Neural Transm Park Dis Dement Sect* 1995;9:73-86.
15. Mori E, Yoneda Y, Yamashita H, et al. Medial temporal structures relate to memory impairment in Alzheimer's disease: an MRI volumetric study. *J Neurol Neurosurg Psychiatr* 1997;63:214-221.
16. Petersen RC, Jack CR Jr, Xu YC, et al. Memory and MRI-based hippocampal volumes in aging and AD. *Neurology* 2000;54:581-587.
17. Bittner D, Gron G, Schirrmeister H, et al. [18F]FDG-PET in patients with Alzheimer's disease: marker of disease spread. *Dement Geriatr Cogn Disord* 2005;19:24-30.
18. Meltzer CC, Zubieta JK, Brandt J, et al. Regional hypometabolism in Alzheimer's disease as measured by positron emission tomography after correction for effects of partial volume averaging. *Neurology* 1996;47:454-461.
19. Bracco L, Bessi V, Piccini C, et al. Metabolic correlates of executive dysfunction: different patterns in mild and very mild Alzheimer's disease. *J Neurol* 2007;254:1052-1065.
20. Kalpouzos G, Eustache F, de la Sayette V, et al. Working memory and FDG-PET dissociate early and late onset Alzheimer disease patients. *J Neurol* 2005;252:548-558.
21. Cabeza R, Nyberg L. Imaging cognition II. An empirical review of 275 PET and fMRI studies. *J Cogn Neurosci* 2000;12:1-47.
22. Eldridge LL, Knowlton BJ, Furmanski CS, et al. Remembering episodes: a selective role for the hippocampus during retrieval. *Nat Neurosci* 2000;3:1149-1152.
23. Lee AC, Robbins TW, Pickard JD, et al. Asymmetric frontal activation during episodic memory: the effects of stimulus type on encoding and retrieval. *Neuropsychologia* 2000;38:677-692.
24. Schacter DL, Wagner AD. Medial temporal lobe activations in fMRI and PET studies of episodic encoding and retrieval. *Hippocampus* 1999;9:7-24.
25. Bunge SA, Burrows B, Wagner AD. Prefrontal and hippocampal contributions to visual associative recognition: interactions between cognitive control and episodic retrieval. *Brain Cogn* 2004;56:141-152.
26. Owen AM, Milner B, Petrides M, et al. Memory for object features versus memory for object location: a positron-emission tomography study of encoding and retrieval processes. *Proc Natl Acad Sci U S A* 1996;93:9212-9217.
27. Shannon BJ, Buckner RL. Functional-anatomic correlates of memory retrieval that suggest nontraditional processing roles for multiple distinct regions within posterior parietal cortex. *J Neurosci* 2004;24:10084-10092.
28. Christoff K, Prabhakaran V, Dorfman J, et al. Rostrolateral prefrontal cortex involvement in relational integration during reasoning. *Neuroimage* 2001;14:1136-1149.
29. Dagher A, Owen AM, Boecker H, Brooks DJ. Mapping the network for planning: a correlational PET activation study with the Tower of London task. *Brain* 1999;122(Pt 10):1973-1987.
30. Prabhakaran V, Smith JA, Desmond JE, et al. Neural substrates of fluid reasoning: an fMRI study of neocortical activation during performance of the Raven's Progressive Matrices Test. *Cognit Psychol* 1997;33:43-63.
31. Grundman M, Petersen RC, Ferris SH, et al. Mild cognitive impairment can be distinguished from Alzheimer disease and normal aging for clinical trials. *Arch Neurol* 2004;61:59-66.
32. Petersen RC. Mild cognitive impairment as a diagnostic entity. *J Intern Med* 2004;256:183-194.
33. Petersen RC, Doody R, Kurz A, et al. Current concepts in mild cognitive impairment. *Arch Neurol* 2001;58:1985-1992.
34. Wechsler D. *Wechsler Memory Scale-revised Manual*. San Antonio, TX: The Psychological Corporation, 1987.
35. Morris JC. The Clinical Dementia Rating (CDR): current version and scoring rules. *Neurology* 1993;43:2412-2414.
36. Lawton MP, Brody EM. Assessment of older people: self-maintaining and instrumental activities of daily living. *Gerontologist* 1969;9:179-186.
37. Mahoney FI, Barthel DW. Functional evaluation: the Barthel Index. *Md State Med J* 1965;14:61-65.

38. Folstein MF, Folstein SE, McHugh PR. "Mini-mental state." A practical method for grading the cognitive state of patients for the clinician. *J Psychiatr Res* 1975;12:189-198.
39. McKhann G, Drachman D, Folstein M, et al. Clinical diagnosis of Alzheimer's disease: report of the NINCDS-ADRDA Work Group under the auspices of Department of Health and Human Services Task Force on Alzheimer's Disease. *Neurology* 1984;34:939-944.
40. Galasko D, Klauber MR, Hofstetter CR, et al. The Mini-Mental State Examination in the early diagnosis of Alzheimer's disease. *Arch Neurol* 1990;47:49-52.
41. Lezak M. *Neuropsychological Assessment*. 3rd ed. New York: Oxford University Press, 1994.
42. Halford GS, Wilson WH, Phillips S. Processing capacity defined by relational complexity: implications for comparative, developmental, and cognitive psychology. *Behav Brain Sci* 1998;21:803-831; discussion 831-864.
43. Raven JC. *Guide to Using the Coloured Progressive Matrices*. London: H.K. Lewis, 1965.
44. Waltz JA, Knowlton BJ, Holyoak KJ, et al. Relational integration and executive function in Alzheimer's disease. *Neuropsychology* 2004;18:296-305.
45. Esposito G, Kirkby BS, Van Horn JD, et al. Context-dependent, neural system-specific neurophysiological concomitants of ageing: mapping PET correlates during cognitive activation. *Brain* 1999;122(Pt 5):963-979.
46. Nagano-Saito A, Washimi Y, Arahata Y, et al. Cerebral atrophy and its relation to cognitive impairment in Parkinson disease. *Neurology* 2005;64:224-229.
47. Baudic S, Barba GD, Thibaudet MC, et al. Executive function deficits in early Alzheimer's disease and their relations with episodic memory. *Arch Clin Neuropsychol* 2006;21:15-21.
48. Lafleche G, Albert MS. Executive function deficits in mild Alzheimer's disease. *Neuropsychology* 1995;9:313-320.
49. Dubois B, Slachevsky A, Litvan I, et al. The FAB. a Frontal Assessment Battery at bedside. *Neurology* 2000;55:1621-1626.
50. Ibanez V, Pietrini P, Alexander GE, et al. Regional glucose metabolic abnormalities are not the result of atrophy in Alzheimer's disease. *Neurology* 1998;50:1585-1593.
51. Salmon E, Lespagnard S, Marique P, et al. Cerebral metabolic correlates of four dementia scales in Alzheimer's disease. *J Neurol* 2005;252:283-290.
52. Chetelat G, Desgranges B, de la Sayette V, et al. Mild cognitive impairment: can FDG-PET predict who is to rapidly convert to Alzheimer's disease? *Neurology* 2003;60:1374-1377.
53. de Leon MJ, Convit A, Wolf OT, et al. Prediction of cognitive decline in normal elderly subjects with 2-[(18)F]fluoro-2-deoxy-D-glucose/poitron-emission tomography (FDG/PET). *Proc Natl Acad Sci U S A* 2001;98:10966-10971.
54. Mosconi L. Brain glucose metabolism in the early and specific diagnosis of Alzheimer's disease. FDG-PET studies in MCI and AD. *Eur J Nucl Med Mol Imaging* 2005;32:486-510.
55. Nestor PJ, Fryer TD, Smielewski P, et al. Limbic hypometabolism in Alzheimer's disease and mild cognitive impairment. *Ann Neurol* 2003;54:343-351.
56. Lopez OL, Becker JT, Jagust WJ, et al. Neuropsychological characteristics of mild cognitive impairment subgroups. *J Neurol Neurosurg Psychiatr* 2006;77:159-165.
57. Bokde AL, Pietrini P, Ibanez V, et al. The effect of brain atrophy on cerebral hypometabolism in the visual variant of Alzheimer disease. *Arch Neurol* 2001;58:480-486.
58. Singh V, Chertkow H, Lerch JP, et al. Spatial patterns of cortical thinning in mild cognitive impairment and Alzheimer's disease. *Brain* 2006;129:2885-2893.
59. Buchert R, Wilke F, Chakrabarti B, et al. Adjusted scaling of FDG positron emission tomography images for statistical evaluation in patients with suspected Alzheimer's disease. *J Neuroimaging* 2005;15:348-355.
60. Mevel K, Desgranges B, Baron JC, et al. Detecting hippocampal hypometabolism in Mild Cognitive Impairment using automatic voxel-based approaches. *Neuroimage* 2007;37:18-25.
61. Bernard FA, Desgranges B, Eustache F,et al. Neural correlates of age-related verbal episodic memory decline: a PET study with combined subtraction/correlation analysis. *Neurobiol Aging* 2007;28:1568-1576.
62. Buckner RL, Petersen SE, Ojemann JG, et al. Functional anatomical studies of explicit and implicit memory retrieval tasks. *J Neurosci* 1995;15:12-29.
63. Guillozet AL, Weintraub S, Mash DC, et al. Neurofibrillary tangles, amyloid, and memory in aging and mild cognitive impairment. *Arch Neurol* 2003;60:729-736.
64. Markesbery WR, Schmitt FA, Kryscio RJ, et al. Neuropathologic substrate of mild cognitive impairment. *Arch Neurol* 2006;63:38-46.
65. Moscovitch C, Kapur S, Kohler S, et al. Distinct neural correlates of visual long-term memory for spatial location and object identity: a positron emission tomography study in humans. *Proc Natl Acad Sci U S A* 1995;92:3721-3725.
66. Johnson SC, Schmitz TW, Moritz CH, et al. Activation of brain regions vulnerable to Alzheimer's disease: the effect of mild cognitive impairment. *Neurobiol Aging* 2006;27:1604-1612.
67. Meguro K, Blaizot X, Kondoh Y, et al. Neocortical and hippocampal glucose hypometabolism following neurotoxic lesions of the entorhinal and perirhinal cortices in the non-human primate as shown by PET. Implications for Alzheimer's disease. *Brain* 1999;122(Pt 8):1519-1531.
68. Meguro K, LeMestric C, Landeau B, et al. Relations between hypometabolism in the posterior association neocortex and hippocampal atrophy in Alzheimer's disease: a PET/MRI correlative study. *J Neurol Neurosurg Psychiatr* 2001;71:315-321.
69. Minoshima S, Giordani B, Berent S, et al. Metabolic reduction in the posterior cingulate cortex in very early Alzheimer's disease. *Ann Neurol* 1997;42:85-94.
70. Carpenter PA, Just MA, Shell P. What one intelligence test measures: a theoretical account of the processing in the Raven Progressive Matrices Test. *Psychol Rev* 1990;97:404-431.
71. Kramer JH, Nelson A, Johnson JK, et al. Multiple cognitive deficits in amnestic mild cognitive impairment. *Dement Geriatr Cogn Disord* 2006;22:306-311.
72. Nordlund A, Rolstad S, Hellstrom P et al. The Goteborg MCI study: mild cognitive impairment is a heterogeneous condition. *J Neurol Neurosurg Psychiatr* 2005;76:1485-1490.
73. Royall DR, Chiodo LK, Polk MJ. Misclassification is likely in the assessment of mild cognitive impairment. *Neuroepidemiology* 2004;23:185-191.
74. Hazeltine E, Bunge SA, Scanlon MD et al. Material-dependent and material-independent selection processes in the frontal and parietal lobes: an event-related fMRI investigation of response competition. *Neuropsychologia* 2003;41:1208-1217.
75. Collette F, Van Der Linden M. Brain imaging of the central executive component of working memory. *Neurosci Biobehav Rev* 2002;26:105-125.
76. Kemppainen NM, Aalto S, Wilson IA, et al. PET amyloid ligand [11C]PIB uptake is increased in mild cognitive impairment. *Neurology* 2007;68:1603-1606.
77. Small GW, Kepe V, Ercoli LM, et al. PET of brain amyloid and tau in mild cognitive impairment. *N Engl J Med* 2006;355:2652-2663.

Original Paper

Cerebrovascular Diseases

Cerebrovasc Dis 2008;26:556–562
DOI: 10.1159/000160213

Received: April 4, 2008
Accepted: June 24, 2008
Published online: October 6, 2008

Statistical Parametric Analysis of Cerebral Blood Flow in Vascular Dementia with Small-Vessel Disease Using ^{99m}Tc-HMPAO SPECT

Hiroki Kato[a] Takuya Yoshikawa[d] Naohiko Oku[e] Masao Imaizumi[a]
Masashi Takasawa[a] Yasuyuki Kimura[a] Katsufumi Kajimoto[a] Makiko Tanaka[b]
Kazuo Kitagawa[c] Masatsugu Hori[b] Jun Hatazawa[a]

Departments of [a]Nuclear Medicine and Tracer Kinetics, [b]Cardiovascular Medicine, [c]Neurology, Osaka University Graduate School of Medicine, Suita, [d]Osaka-Minami Medical Center, Kawachinagano, and [e]Department of Nuclear Medicine, Hyogo College of Medicine, Nishinomiya, Japan

Key Words
Vascular dementia · Subcortical arteriosclerotic encephalopathy · Single photon emission computed tomography · Cerebrovascular circulation

Abstract
Background: Subcortical ischemic vascular dementia (SVD) caused by small-artery disease is a major cause of dementia. It still remains unclear, however, whether SVD may present with localized regional cerebral blood flow (rCBF) changes. We aimed to clarify the local rCBF changes associated with dementia in patients with early-stage SVD. ***Methods:*** The subjects consisted of 15 patients with early-stage SVD [Mini Mental State Examination (MMSE) score: 20 ± 3.5] without apparent brain atrophy (SVD group), 11 patients without dementia with white matter lesions (non-dementia-WML group) and 16 age-matched controls. All the subjects were right-handed and underwent brain perfusion single photon emission computed tomography (SPECT), magnetic resonance imaging and cognitive function testing. Statistical analysis of the differences in the SPECT rCBF was performed by SPM2. The degree of severity of the WMLs was evaluated based on the Scheltens rating scale. ***Results:*** The results of SPM analysis revealed that the rCBF in the SVD group was significantly decreased in the pulvinar nuclei of the thalamus of both sides as compared with that in the controls, and in the left pulvinar nucleus as compared with that in the non-dementia-WML group. On the other hand, SPM analysis revealed no significant reduction in rCBF in the non-dementia-WML group as compared with that in the controls. The WMLs in the left parietal region were severer in the SVD group than in the non-dementia-WML group. ***Conclusions:*** In patients with early-stage SVD without apparent brain atrophy, significant rCBF reduction in the bilateral pulvinar nuclei as compared with that in normal controls, and in the left pulvinar nucleus as compared with that in patients without dementia with WMLs was found.

Introduction

Subcortical ischemic vascular dementia (SVD) due to small-artery disease and hypoperfusion is one of the major causes of cognitive impairment and dementia [1, 2].

KARGER
Fax +41 61 306 12 34
E-Mail karger@karger.ch
www.karger.com

1015–9770/08/0265–0556$24.50/0

Accessible online at:
www.karger.com/ced

Hiroki Kato, MD, PhD
Department of Nuclear Medicine and Tracer Kinetics
Osaka University Graduate School of Medicine, 2-2 Yamadaoka
Suita 565-0871 (Japan)
Tel. +81 6 6879 3461, Fax +81 6 6879 3469, E-Mail kato-h@umin.ac.jp

Localized reduction of the regional cerebral blood flow (rCBF) in the posterior cingulate and parietotemporal region of the brain has been reported previously in cases of mild Alzheimer's disease [3]. While very few studies have focused on the localized rCBF changes in cases of SVD [4, 5], our previous study revealed that in cases of mild SVD, the rCBF distribution is more heterogeneous than that in healthy controls [6]. The purpose of the present study was to clarify the localized rCBF changes associated with dementia in patients with subcortical ischemic lesions.

Materials and Methods

Subjects

The subjects consisted of 15 patients (5 men, 10 women) with early-stage SVD (SVD group), 11 patients (6 men, 5 women) with white matter lesions (WMLs) on T_2-weighted magnetic resonance imaging (MRI) but no dementia (non-dementia-WML group) (table 1), and 16 age-matched healthy volunteers (5 men, 11 women, mean age ± SD, 66 ± 9.0 years; control group). The present study was a secondary retrospective analysis of our previous studies in which we compared the CBF between patients with vascular dementia and those with Alzheimer's disease [6, 7]. In this study, therefore, all the subjects of the SVD group and the normal controls were selected from the patients included in the previous study [6]. In order to select patients with early-stage SVD, only the subjects who had no apparent brain atrophy by visual assessment or had more than 70% normalized parenchymal volume as evaluated by the volumetric method described later were included in the present study. This criterion is reasonable for the analysis, because atrophic brains are subject to misregistration or inadequate anatomical normalization by the Statistical Parametric Mapping (SPM) software (Wellcome Department of Cognitive Neurology, London, UK) [8], and CBF in the deep brain structures is strongly influenced by artifacts and cannot be assessed correctly by SPM in such cases. As described in the previous papers, the NINDS-AIREN criteria [9], the *Diagnostic and Statistical Manual of Mental Disorders* [10], Hachinski's ischemic score [11], and Erkinjuntti's criteria [12] were used for making the diagnosis of SVD in our studies to ensure comprehensive examination. The clinical features of vascular dementia included sudden onset, stepwise progression, prolonged plateaus, periods of spontaneous improvement, and onset or worsening with the development of stroke or episodes of hypoperfusion. The soft focal neurologic signs/symptoms strongly supported the diagnosis of vascular dementia. Subtype classifications of vascular dementia were based on the results of neuroimaging and clinical evaluation [12]. Probable vascular dementia was diagnosed in all the patients of the SVD group, and all were classified as having small-vessel disease based on the presence of small white matter hyperintensities or lacunae in the deep white matter, basal ganglia and thalamus on T_2-weighted MR images with no obvious lesions in the cortex. The 11 patients of the non-dementia-WML group were newly selected in this study from among the outpatients at our hospital who met the criteria mentioned above, except for the manifestation of cognitive impairment. The healthy volunteers did not present any abnormal findings on CBF single photon emission computed tomography (SPECT) or on CT and MRI, and/or no evident neuropsychologic abnormalities as assessed by a full clinical examination, including history taking, neuropsychologic tests and neurologic examinations. The Mini Mental State Examination (MMSE) [13] was performed within 3 months of the CBF SPECT to evaluate the cognitive function in these subjects. The dementia status of the patients of the SVD group was also evaluated using the revised Hasegawa dementia scale (score: 19.5 ± 3.8) [14]. Patients who could not undergo the cognitive function testing because of such conditions as aphasia were excluded from the study. All of the subjects were right-handed, and all underwent CBF SPECT between June 2000 and May 2005. Informed consent was obtained from all of the subjects or from the closest family members when a subject could not fully understand the explanation given about the study. The clinical characteristics of the two patient groups are described in table 1.

Table 1. Clinical characteristics of the patients

	SVD group (n = 15)	Non-dementia-WML group (n = 11)	p
M/F	5/10	6/5	0.259
Age (mean ± SD), years	69 ± 8.4	65 ± 13	0.384
Hypertension, %	79	64	0.536
Hyperlipidemia, %	50	36	0.572
Diabetes mellitus, %	38	9	0.228
Smoking, %	29	22	0.829
Statin use, %	20	9	0.646
ACE inhibitor or ARB use, %	29	36	0.767
MMSE score	20 ± 3.5	29 ± 1.2	<0.001

ACE = Angiotensin-converting enzyme; ARB = angiotensin II receptor blocker.

SPECT Data Acquisition

The protocol for the SPECT data acquisition was the same as that in our previous studies [6, 7]. In brief, technetium-99m hexamethyl propyleneamine oxime (^{99m}Tc-HMPAO) was produced by reconstituting HMPAO with 20 mCi (740 MBq) of fresh ^{99m}Tc pertechnetate, and injected intravenously before the scanning. SPECT scanning was performed with a four-headed gamma camera (Gamma View SPECT 2000H; Hitachi Medical Corp., Tokyo, Japan) using a low-energy thin-section parallel-hole collimator [15]. The projection data were prefiltered with a Butterworth filter (cutoff frequency 0.20 cycles/pixel, order 10) and reconstructed into transaxial images of 4.0-mm-thick sections in planes parallel to the orbitomeatal line. Chang's [16] attenuation correction was applied to the reconstructed data using an attenuation coefficient of 0.08 cm^{-1}.

SPM Analysis

Analysis was carried out on a personal computer DELL Dimension 8300 (DELL Inc., Tex., USA) with Microsoft Windows

XP (Microsoft Corp., Wash., USA) as the operating system using the SPM software, version SPM2 (http://www.fil.ion.ucl.ac.uk/spm), implemented in MATLAB (Mathworks Inc., Mass., USA).

The SPECT images of each subject were normalized to the Montreal Neurological Institute (MNI) template space with minimal changes of the 12 affine parameters that were associated with spatial distortion [17]. The results of the special normalization were checked with the 'Check Registration' tool in SPM2 to confirm the accuracy of the rigid or nonlinear transformation. All the images of a brain section were sampled and averaged to arrive at the mean pixel intensity for that image. The intensity threshold was set at 60% of the whole-brain mean to enable detection of CBF change in the deep white matter. The global CBF rate was normalized to an arbitrary mean of 50/100 ml of brain volume per minute. The images were smoothed with a three-dimensional isotropic Gaussian kernel of 12 mm full-width at half maximum. The SPM statistical model performed voxel-by-voxel two-sampled t tests to compare each pair of groups. As for each test, the resultant set of voxel values constituted a statistical parametric map of the t statistic SPM{t}. The significance threshold was set at $p < 0.001$ (uncorrected) for the peak height for screening purposes. Only clusters with a size greater than 50 voxels were tested for significance. The criteria to identify statistically significant clusters were set at $p < 0.05$, after correcting for multiple comparisons [18]. Moreover, voxel-by-voxel linear regression between the MMSE scores and whole-brain rCBF was generated using SPM2. The significance threshold was set at $p < 0.01$, uncorrected, assuming a cluster of at least 20 suprathreshold voxels.

Evaluation of WMLs

All the patients underwent SPECT and MRI within an interval of 3 months. Scans were obtained on the following scanners: Genesis Signa 1.5T (GE Yokogawa Medical Systems Ltd., Tokyo, Japan), Signa Excite 1.5T (GE), and Magnetom Vision 1.5T (Siemens AG, Erlangen, Germany). The MR protocol included T_2-weighted two-dimensional fast spin echo sequences (scan parameters: axial plane, FOV 250 mm, matrix 256 × 256 or 512 × 512, slice thickness 5 mm, interslice gap 1–1.5 mm, TE 90–131 ms, TR 4,500–5,000 ms).

The degree of severity of the WMLs was rated visually on axial T_2-weighted images based on the Scheltens rating scale [19] by a single rater who was blinded to the clinical details. The Scheltens rating scale, which evaluates the presence and extent of periventricular lesions (PVLs) and deep white matter lesions (DWMLs) in different anatomic regions on a 0- to 6-point scale, accounts separately for PVLs and DWMLs. In this study, we applied this scale to supratentorial regions separately in each hemisphere. Scores for DWMLs of 0–6 were assigned in 4 subcortical regions (frontal, parietal, occipital, and temporal lobes) and 5 basal ganglia regions (the caudate nucleus, putamen, globus pallidus, thalamus, and internal capsule) in each hemisphere. A score of 0 was assigned when no DWML was found. If the largest lesion in a region was smaller than 4 mm, a score of 1 was assigned when there were no more than 5 lesions, and a score of 2 was assigned when there were more than 5 lesions. If the largest lesion was between 4 and 10 mm, a score of 3 was given when there were no more than 5 lesions, while a score of 4 was given when there were more than 5 lesions. A score of 5 represented the presence of the largest lesions of 10 mm or more. A score of 6 denoted the presence of confluent lesions. For PVLs [frontal (caps), occipital (caps), along the ventricles (bands)], scores of 0–2 were assigned. A score of 0 was assigned to the absence of PVLs, a score of 1 was assigned to a smooth halo that extended not more than 5 mm, and a score of 2 was assigned to confluent lesions larger than 5 mm. All the regional WML scores were summed up as the total WML score for each patient.

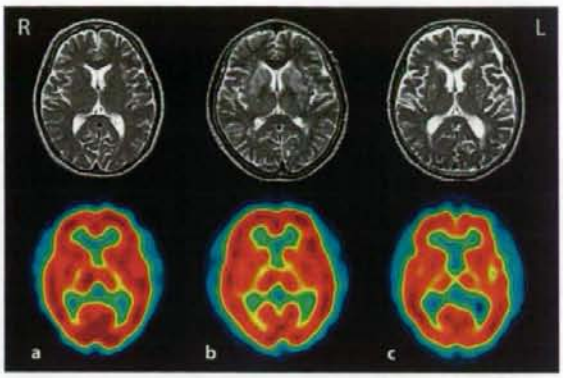

Fig. 1. A representative case from each group. The upper images are T_2-weighted MR images and the lower images are SPECT images. **a** A 61-year-old female control subject. **b** A 63-year-old female patient with WMLs but no dementia. **c** An 82-year-old man with SVD due to small-artery disease.

Volumetry

The extent of cerebral atrophy was assessed by volumetric measures normalized for a total intracranial area on 5 T_2-weighted axial slices. The volumetry was carried out semiautomatically on a personal computer with the use of public domain ImageJ software (http://rsb.info.nih.gov/ij/), as described by Ihara et al. [20]. In brief, we manually outlined the inner boundary of the calvarium on T_2-weighted axial images to determine the total intracranial area. The images were then binarized with the intensity threshold set at 60% of mean intracranial pixel values within the outlined area. After the ventricular and subdural areas were semiautomatically outlined with the wand tool, the total number of pixels in each area in the 5 slices was divided by that in the total intracranial area to calculate normalized ventricular and subdural areas. Finally, subtraction of the normalized ventricular and subdural areas from the total intracranial area (value 1.0) yielded normalized parenchymal area.

Data Analysis

Intergroup differences in the mean values of parameters were analyzed using the Mann-Whitney U test by SPSS version 11.0.1 (http://www.SPSS.com). A p value of <0.05 was considered to represent significant difference, whereas a value of between 0.05 and 0.10 was taken as an indicator of mild difference.

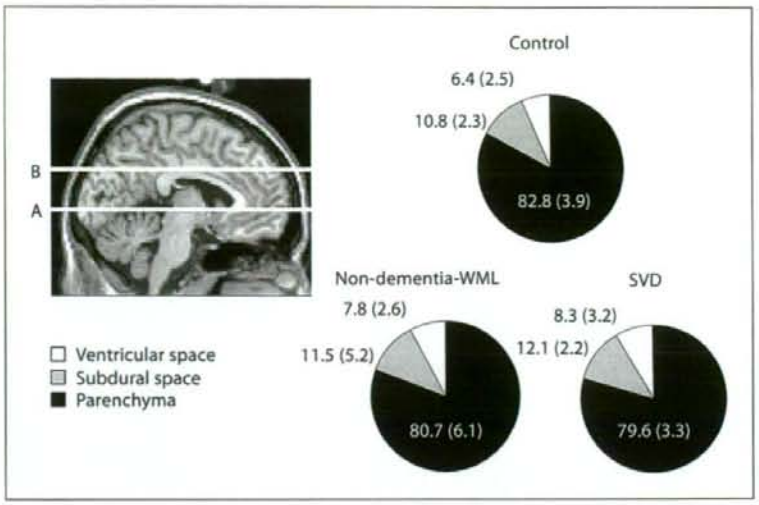

Fig. 2. Comparison of regional brain volumetry among the normal control and the two patient groups (SVD and non-dementia-WML patients). Brain atrophy was assessed on the 5 axial slices of MR images included in the space between the axial AC-PC plane A and B; Montreal Neurological Institute (MNI) coordinate Z = 0 (A) and Z = 30 (B). Regions occupied by brain parenchyma, subdural space, and ventricular space in the 5 slices are averaged and indicated as the ratio to the total intracranial area. Data are mean percentage with SD in parentheses.

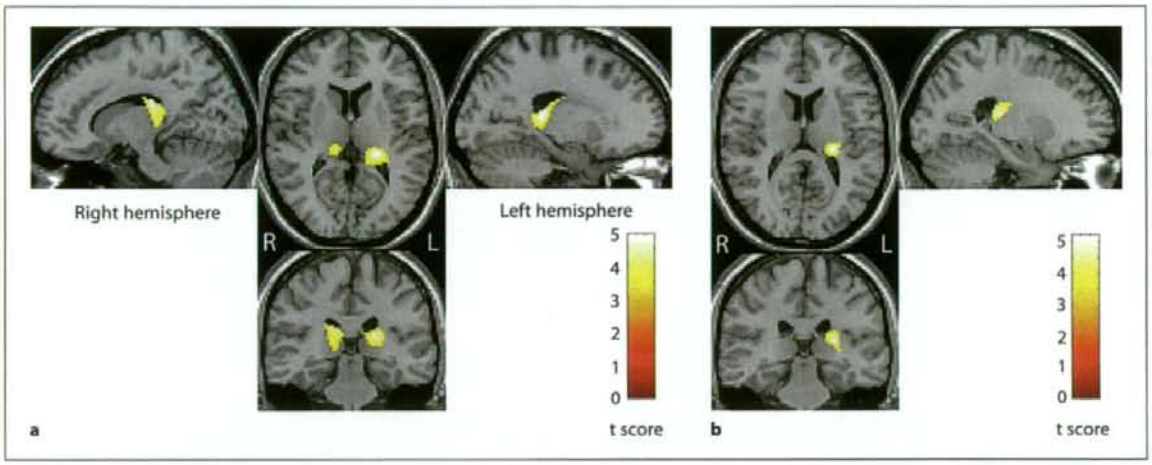

Fig. 3. a Comparisons of the rCBF between patients with SVD and normal controls were performed using SPM2. Significant localized rCBF reductions were detected in the thalami of both sides in the patients with SVD. The cluster on the right side chiefly consisted of the lateral dorsal nucleus and the pulvinar nucleus. The one on the left was mostly made up of the pulvinar nucleus. **b** Comparisons of rCBF were carried out between the patients with SVD and non-dementia-WML patients using SPM2 under the same conditions as those for the above comparisons. The height and the extent threshold for displaying the SPM results map were also the same. Localized rCBF reduction was found in the left thalamus in the patients with SVD. The detected cluster was located in almost the same region as the cluster on the left side described above.

Results

The MR images and SPECT images of representative cases are shown in figure 1. As a result of the volumetry, no significant intergroup differences were shown in brain parenchymal, ventricular, and subdural areas in the 5 axial MR images (fig. 2). The results of SPM analysis revealed that the normalized rCBF in the SVD group was decreased in the thalamus of both sides as compared with that in the controls (fig. 3a), and in the

Table 2. Brain regions with reduction of the rCBF in patients with SVD

Comparison	Anatomic region	MNI coordinates, mm			Cluster size mm^3	t score	Cluster level p (corrected)
		x	y	z			
SVD vs. control	left thalamus (pulvinar)	−20	−32	10	4,392	4.91	0.02
	right thalamus (lateral dorsal nucleus)	12	−24	17	3,472	4.72	0.04
SVD vs. non-dementia-WML	left thalamus (pulvinar)	−21	−25	14	2,568	5.55	0.01

thalamus of the left side as compared with that in the non-dementia-WML group (fig. 3b). In the former comparison, the detected cluster with reduced rCBF in the right thalamus included the dorsal lateral nucleus and the pulvinar nucleus. In both comparisons, the clusters with significant rCBF reduction in the left thalamus contained the pulvinar nucleus (table 2). On the other hand, under the same conditions of SPM analysis as mentioned above, no significant reduction in the rCBF was detected in the patients in the non-dementia-WML group as compared with that in the controls. The WMLs in the left parietal lobe were significantly severer in the SVD group than in the non-dementia-WML group, although there were no significant differences in the overall severity of the WMLs (table 3). No WMLs were found in the thalamic regions showing reduced rCBF in the SVD group as compared with the normal controls or the non-dementia-WML group. There was no significant difference in the average number of lacunae with a diameter of more than 5 mm between the SVD group (0.36 ± 0.67, maximum diameter: 12 mm) and non-dementia-WML group (0.5 ± 0.71, maximum diameter: 11 mm). In the SVD group, a mild correlation between the MMSE score and the rCBF was detected in a small cluster of voxels in the left frontopolar area (Brodmann area 10) (fig. 4).

Table 3. Visual assessment of WMLs based on the Scheltens rating scale

WML type	Region	Side	WML scores (Scheltens)		p
			non-dementia-WML	SVD	
DWML	frontal	R	4.2 ± 1.7	4.6 ± 1.8	NS
		L	4.7 ± 1.6	4.6 ± 2.0	NS
	parietal	R	2.4 ± 2.4	3.9 ± 2.3	NS
		L	2.4 ± 1.7	4.4 ± 1.9	0.02
	temporal	R	3.7 ± 1.8	3.1 ± 2.5	NS
		L	3.2 ± 1.9	3.4 ± 2.2	NS
	occipital	R	4.2 ± 2.2	2.8 ± 2.8	NS
		L	3.6 ± 2.4	3.3 ± 2.7	NS
	caudate	R	0.9 ± 1.9	0.8 ± 1.5	NS
		L	1.0 ± 1.8	0.3 ± 0.9	NS
	putamen	R	2.7 ± 2.3	1.5 ± 1.8	NS
		L	2.4 ± 2.5	1.8 ± 2.2	NS
	globus pallidus	R	0.4 ± 0.7	0.2 ± 0.4	NS
		L	0.3 ± 0.7	0.1 ± 0.3	NS
	internal capsule	R	0.1 ± 0.3	0.6 ± 1.0	NS
		L	0.1 ± 0.4	0.4 ± 0.9	NS
	mean		2.5 ± 1.1	2.5 ± 1.2	NS
PVL	frontal (cap)	R	1.6 ± 0.5	1.7 ± 0.6	NS
		L	1.7 ± 0.5	1.5 ± 0.7	NS
	occipital (cap)	R	1.5 ± 0.5	1.4 ± 0.8	NS
		L	1.5 ± 0.5	1.5 ± 0.8	NS
	along the ventricles (bands)	R	1.5 ± 0.5	1.3 ± 0.6	NS
		L	1.5 ± 0.5	1.3 ± 0.6	NS
	mean		1.6 ± 0.3	1.5 ± 0.6	NS
Total WML score			54 ± 22	54 ± 24	NS

NS = Not significant.

Discussion

Our study revealed a significant reduction in the rCBF in the pulvinar nucleus of both sides and the right dorsal lateral nucleus in the thalamus in patients with early-stage SVD without apparent atrophy as compared with normal controls. A significant correlation was found between the MMSE score and the rCBF in the left frontopolar area (Brodmann area 10) in the SVD group. These results suggest marked reduction of the rCBF in the thalamus in mild SVD, although the rCBF reduction in the frontal area became more prominent as the cognitive decline progressed.

The pulvinar nucleus has been shown to be involved in attention [21], memory [22] and language [23], which are known to be impaired in SVD [24]. According to the

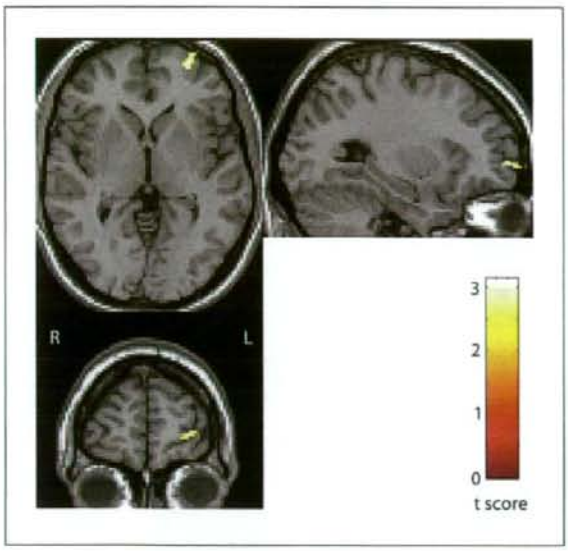

Fig. 4. Voxel-by-voxel linear regression analysis to determine the relation between MMSE scores and whole-brain rCBF in patients with SVD, performed using SPM2. The detected cluster was located in the left frontopolar region (Brodmann area 10).

thalamic connectivity atlas (http://www.fmrib.ox.ac.uk/connect/) constructed based on the classification technique using a probabilistic tractography algorithm with diffusion imaging data [25, 26], the regions in the thalamus showing reduced rCBF in the SVD group as compared with the normal controls or the non-dementia-WML group in the present study were demonstrated to have thalamocortical connections with the prefrontal, parietal and temporal lobes. The rCBF changes in the thalamic nuclei detected by the SPM analysis seemed to be caused not by focal ischemic lesions but by functional inactivation of these regions, because no WMLs were found in these thalamic regions in the SVD group. We speculated that disconnections of thalamocortical and cortico-thalamo-cortical signal circuits may accumulate in SVD, resulting in functional rCBF reduction and decline of cognitive functions. It has been suggested that cerebral remote effects, commonly referred to as diaschisis, caused by small ischemic lesions located in cortico-thalamic and thalamocortical tracts may contribute to decreased cortical metabolic activity and cognitive dysfunction [27, 28].

The functional rCBF changes per voxel caused by these disconnections are thought to be amplified in the thalamus because of the concentration of neuronal fibers [29]. Therefore, the CBF change per voxel in the cluster in the thalamus was evaluated as significant by voxel-based analysis, while heterogeneously distributed rCBF changes in the white matter or cortices [6, 7] were not detected as significant focal reduction by the SPM analysis in the cases with early-stage SVD.

In the present study, significant localized rCBF reduction in the left pulvinar nucleus was demonstrated in the SVD group as compared with the non-dementia-WML group. In addition, the WMLs in the left parietal lobe were significantly severer in the SVD group than in the non-dementia-WML group. This result may support our speculation mentioned above, because a high probability of neuronal connections of the parietal cortex with the ipsilateral pulvinar has been shown [26]. The disruption of the connection between the left parietal cortex and the thalamus may not be the unique cause of dementia in patients with SVD. The relatively preserved connectivity between the parietal cortex and the thalamus in the non-dementia-WML group, however, can be thought as compensating for other neuronal projections disrupted by the WMLs to prevent cognitive decline.

Yang et al. [4] reported that in the patients with SVD, the CBF was decreased in multiple cortical regions, especially around the sylvian fissures or lateral ventricles and the caudate nucleus, in addition to the thalamus. In their study, unlike in our present study, the effects of brain atrophy in patients with dementia were not evaluated or excluded, and it was not clear whether or not the spatial normalization by SPM2 was adequate. Thus, possible misregistration or inadequate spatial normalization of atrophied brains by SPM2 may be one reason for the inconsistency of the results.

There are several limitations to this study. Firstly, in the present study, the rCBF changes related to brain atrophy were not included in the analysis. If such rCBF changes associated with apparent regional brain volume loss were included in the analysis, the thalamus might not be the sole area exhibiting localized rCBF reduction associated with cognitive decline in SVD. Such structural brain change, however, should be evaluated using other methods, like voxel-based morphometry. Secondly, the severity of WMLs was assessed not by an automated method, but by visual evaluation based on the Scheltens rating scale. Although visual assessment may be less objective than automated volumetric methods, the Scheltens visual rating scale has been demonstrated to show good concordance with volumetric methods and to be sufficient for evaluating the severity of WMLs [30].

Conclusions

In patients with early-stage SVD without apparent brain atrophy, localized rCBF reduction in the pulvinar nuclei of the thalami of both sides was found as compared with normal controls, and localized rCBF reduction in the left pulvinar nucleus was found as compared with patients in the non-dementia-WML group.

Acknowledgments

We thank Mr. Yukio Nakamura and the staff of the Department of Nuclear Medicine and the Cyclotron staff of Osaka University Hospital for their technical support in performing the studies. This study was supported by the Molecular Imaging Program on 'Research Base for Exploring New Drugs' of the Ministry of Education, Culture, Sports, Science, and Technology (MEXT), Japan.

References

1 Roman GC, Erkinjuntti T, Wallin A, Pantoni L, Chui HC: Subcortical ischaemic vascular dementia. Lancet Neurol 2002;1:426–436.
2 Erkinjuntti T: Vascular cognitive deterioration and stroke. Cerebrovasc Dis 2007; 24(suppl 1):189–194.
3 Ishii K, Sasaki M, Yamaji S, Sakamoto S, Kitagaki H, Mori E: Demonstration of decreased posterior cingulate perfusion in mild Alzheimer's disease by means of $H_2{}^{15}O$ positron emission tomography. Eur J Nucl Med 1997;24:670–673.
4 Yang DW, Kim BS, Park JK, Kim SY, Kim EN, Sohn HS: Analysis of cerebral blood flow of subcortical vascular dementia with single photon emission computed tomography: adaptation of statistical parametric mapping. J Neurol Sci 2002;203–204:199–205.
5 Shim YS, Yang DW, Kim BS, Shon YM, Chung YA: Comparison of regional cerebral blood flow in two subsets of subcortical ischemic vascular dementia: statistical parametric mapping analysis of SPECT. J Neurol Sci 2006;250:85–91.
6 Yoshikawa T, Murase K, Oku N, Kitagawa K, Imaizumi M, Takasawa M, Nishikawa T, Matsumoto M, Hatazawa J, Hori M: Statistical image analysis of cerebral blood flow in vascular dementia with small-vessel disease. J Nucl Med 2003;44:505–511.
7 Yoshikawa T, Murase K, Oku N, Imaizumi M, Takasawa M, Rishu P, Kimura Y, Ikejiri Y, Kitagawa K, Hori M, Hatazawa J: Heterogeneity of cerebral blood flow in Alzheimer disease and vascular dementia. AJNR Am J Neuroradiol 2003;24:1341–1347.
8 Ishii K, Willoch F, Minoshima S, Drzezga A, Ficaro EP, Cross DJ, Kuhl DE, Schwaiger M: Statistical brain mapping of ^{18}F-FDG PET in Alzheimer's disease: validation of anatomic standardization for atrophied brains. J Nucl Med 2001;42:548–557.
9 Roman GC, Tatemichi TK, Erkinjuntti T, Cummings JL, Masdeu JC, Garcia JH, Amaducci L, Orgogozo JM, Brun A, Hofman A, et al: Vascular dementia: diagnostic criteria for research studies. Report of the NINDS-AIREN International Workshop. Neurology 1993;43:250–260.
10 American Psychiatric Association: Diagnostic and Statistical Manual of Mental Disorders, ed 4. Washington, American Psychiatric Association, 1994.
11 Hachinski VC, Iliff LD, Zilhka E, Du Boulay GH, McAllister VL, Marshall J, Russell RW, Symon L: Cerebral blood flow in dementia. Arch Neurol 1975;32:632–637.
12 Erkinjuntti T, Inzitari D, Pantoni L, Wallin A, Scheltens P, Rockwood K, Roman GC, Chui H, Desmond DW: Research criteria for subcortical vascular dementia in clinical trials. J Neural Transm Suppl 2000;59:23–30.
13 Folstein MF, Folstein SE, McHugh PR: 'Mini-mental state'. A practical method for grading the cognitive state of patients for the clinician. J Psychiatr Res 1975;12:189–198.
14 Katou S, Simogai H, Hasegawa K: Development of the revised version of Hasegawa's dementia scale (HDS-R). Jpn J Geriatr Psychiatry 1991;2:1339–1342.
15 Kimura K, Hashikawa K, Etani H, Uehara A, Kozuka T, Moriwaki H, Isaka Y, Matsumoto M, Kamada T, Moriyama H, et al: A new apparatus for brain imaging: four-head rotating gamma camera single-photon emission computed tomograph. J Nucl Med 1990;31: 603–609.
16 Chang LT: A method for attenuation correction in radionuclide computed tomography. IEEE Trans Nucl Sci 1978;25:638–643.
17 Friston KJ, Ashburner J, Frith CD, Poline JB, Heather RS, Frackowiak RSJ: Spatial registration and normalization of images. Hum Brain Mapp 1995;3:165–189.
18 Friston KJ, Holmes A, Poline JB, Price CJ, Frith CD: Detecting activations in PET and fMRI: levels of inference and power. Neuroimage 1996;4:223–235.
19 Scheltens P, Barkhof F, Leys D, Pruvo JP, Nauta JJ, Vermersch P, Steinling M, Valk J: A semiquantative rating scale for the assessment of signal hyperintensities on magnetic resonance imaging. J Neurol Sci 1993;114:7–12.
20 Ihara M, Tomimoto H, Ishizu K, Mukai T, Yoshida H, Sawamoto N, Inoue M, Doi T, Hashikawa K, Konishi J, Shibasaki H, Fukuyama H: Decrease in cortical benzodiazepine receptors in symptomatic patients with leukoaraiosis: a positron emission tomography study. Stroke 2004;35:942–947.
21 Shipp S: The brain circuitry of attention. Trends Cogn Sci 2004;8:223–230.
22 Johnson MD, Ojemann GA: The role of the human thalamus in language and memory: evidence from electrophysiological studies. Brain Cogn 2000;42:218–230.
23 Ojemann GA: Asymmetric function of the thalamus in man. Ann NY Acad Sci 1977; 299:380–396.
24 O'Brien JT, Erkinjuntti T, Reisberg B, Roman G, Sawada T, Pantoni L, Bowler JV, Ballard C, DeCarli C, Gorelick PB, Rockwood K, Burns A, Gauthier S, DeKosky ST: Vascular cognitive impairment. Lancet Neurol 2003; 2:89–98.
25 Behrens TE, Johansen-Berg H, Woolrich MW, Smith SM, Wheeler-Kingshott CA, Boulby PA, Barker GJ, Sillery EL, Sheehan K, Ciccarelli O, Thompson AJ, Brady JM, Matthews PM: Non-invasive mapping of connections between human thalamus and cortex using diffusion imaging. Nat Neurosci 2003;6:750–757.
26 Johansen-Berg H, Behrens TE, Sillery E, Ciccarelli O, Thompson AJ, Smith SM, Matthews PM: Functional-anatomical validation and individual variation of diffusion tractography-based segmentation of the human thalamus. Cereb Cortex 2005;15:31–39.
27 Tatemichi TK, Desmond DW, Prohovnik I: Strategic infarcts in vascular dementia. A clinical and brain imaging experience. Arzneimittelforschung 1995;45:371–385.
28 Chukwudelunzu FE, Meschia JF, Graff-Radford NR, Lucas JA: Extensive metabolic and neuropsychological abnormalities associated with discrete infarction of the genu of the internal capsule. J Neurol Neurosurg Psychiatry 2001;71:658–662.
29 Pawlak M, Krejza J: A new visual scale to assess white matter hyperintensities within cholinergic pathways. Stroke 2005;36:2064–2065.
30 Gouw AA, Van der Flier WM, van Straaten EC, Barkhof F, Ferro JM, Baezner H, Pantoni L, Inzitari D, Erkinjuntti T, Wahlund LO, Waldemar G, Schmidt R, Fazekas F, Scheltens P: Simple versus complex assessment of white matter hyperintensities in relation to physical performance and cognition: the LADIS study. J Neurol 2006;253:1189–1196.

Original Paper

Cerebrovascular Diseases

Cerebrovasc Dis 2008;26:9–15
DOI: 10.1159/000135647

Received: October 11, 2007
Accepted: January 4, 2008
Published online: May 30, 2008

Cerebral Hemodynamics and Oxygen Metabolism in Patients with Moyamoya Syndrome Associated with Atherosclerotic Steno-Occlusive Arterial Lesions

Hiroki Kato[a] Eku Shimosegawa[a] Naohiko Oku[d] Yasuyuki Kimura[a]
Katsufumi Kajimoto[a] Makiko Tanaka[a] Masatsugu Hori[b] Kazuo Kitagawa[c]
Jun Hatazawa[a]

Departments of [a]Nuclear Medicine and Tracer Kinetics, [b]Cardiovascular Medicine and [c]Neurology, Osaka University Graduate School of Medicine, Suita, and [d]Department of Nuclear Medicine, Hyogo College of Medicine, Nishinomiya, Japan

Key Words
Moyamoya syndrome · Atherosclerosis · Cerebrovascular disease · Chronic cerebral ischemia · Cerebral blood flow · Intracranial arterial stenosis

Abstract
Background: Patients with major cerebral artery steno-occlusion and the formation of the moyamoya-like vessels associated with some other disorders have been distinguished from moyamoya disease and classified as moyamoya syndrome. The hemodynamic and metabolic backgrounds of the moyamoya syndrome associated with atherosclerosis have not yet been investigated. We aimed to elucidate the hemodynamic and metabolic characteristics associated with the development of basal moyamoya-like vessels in moyamoya syndrome with atherosclerosis. ***Methods:*** Twenty-one patients with chronic unilateral atherosclerotic steno-occlusive lesions of the internal carotid artery or middle cerebral artery (MCA) were enrolled in the study. Based on the angiographic findings, the patients were classified into 2 groups: the moyamoya syndrome group (n = 7) and the non-moyamoya-syndrome group (n = 14). We conducted angiographic evaluations of the extent of the development of basal moyamoya-like vessels in the moyamoya syndrome group. The cerebral blood flow, cerebral metabolic rate of oxygen, oxygen extraction fraction (OEF) and cerebral blood volume were measured using PET in the ipsilateral MCA area in the patients and in normal controls (n = 6). ***Results:*** The OEF in the ipsilateral MCA area, except in the basal ganglia, was significantly higher in the moyamoya syndrome group than in the non-moyamoya-syndrome group ($p < 0.001$). The extent of the development of basal moyamoya-like vessels was closely correlated with the elevation of the OEF ($r > 0.999$, $p < 0.001$). ***Conclusion:*** The basal moyamoya-like vessels are evidence of misery perfusion in patients with unilateral chronic atherosclerotic steno-occlusive lesions of major cerebral artery trunks.

Introduction

Moyamoya vessels in the basal ganglia region are one of the most characteristic findings on cerebral angiography in moyamoya disease [1]. Previous studies have sug-

KARGER
Fax +41 61 306 12 34
E-Mail karger@karger.ch
www.karger.com

1015–9770/08/0261–0009$24.50/0

Accessible online at:
www.karger.com/ced

Jun Hatazawa, MD, PhD
Department of Nuclear Medicine and Tracer Kinetics, Osaka University Graduate School of Medicine, 2-2 Yamadaoka Suita
Osaka 565-0871 (Japan)
Tel. +81 6 6879 3461, Fax +81 6 6879 3469, E-Mail hatazawa@tracer.med.osaka-u.ac.jp

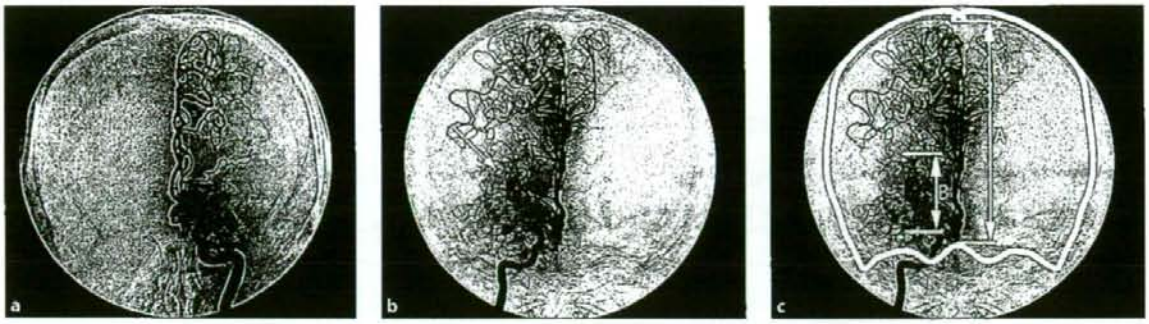

Fig. 1. Representative DSA images in the 2 patient groups. **a** Anteroposterior-view DSA image of patient No. 15 with left MCA occlusion. No apparent dilated angiographic basal moyamoya vessels are visualized (non-moyamoya-syndrome group). **b** The same view of patient No. 3 with right MCA occlusion. The arrow shows basal moyamoya-like vessels extending from the vicinity of the occlusive lesion to the ipsilateral basal ganglia (moyamoya syndrome group). **c** The extension index of the basal moyamoya-like vessels was calculated as the distance from the root to the top-end of the basal moyamoya-like vessels (B) divided by the distance from the base of the skull (top of the sella turcica) to the top of the skull (A).

gested that the development of moyamoya vessels in moyamoya disease is associated with the presence of severe hemodynamic impairment [2, 3]. On the other hand, patients with systemic disorders such as atherosclerosis also sometimes display angiographic features similar to those of moyamoya disease. Such symptoms are distinguished from moyamoya disease and have been classified as 'moyamoya syndrome' [4]. Only a few papers focusing on moyamoya syndrome associated with atherosclerosis have been published [5, 6], and the relationship between the development of moyamoya-like vascular abnormalities and cerebral hemodynamics has not yet been investigated. The aim of this study was to elucidate the hemodynamic and metabolic changes associated with the development of moyamoya-like vascular abnormalities in patients with moyamoya syndrome associated with unilateral atherosclerotic steno-occlusive disease of the internal carotid or middle cerebral arteries (MCA) in the chronic phase.

Patients and Methods

Patients

All the patients were seen at the Osaka University Medical School Hospital between August 2000 and December 2002, or between April 2004 and July 2006. Twenty-one patients (10 males and 11 females; mean age ± SD = 66 ± 9.0 years) who met the following criteria were included in this study: (1) the presence of atherosclerotic arterial changes of the carotid or the major cerebral arteries (e.g. plaques or intima-media thickening as detected by carotid ultrasonography, or arterial wall irregularities as detected by magnetic resonance angiography or brain angiography); (2) the presence of unilateral chronic atherosclerotic steno-occlusive lesions of the internal carotid artery (ICA; >90% diameter reduction according to the North American Symptomatic Carotid Endarterectomy Trial criteria [7]) or MCA M1 trunk (>80% diameter reduction) accessed by digital subtraction angiography (DSA); (3) independence in their daily life (modified Rankin Scale <3); (4) a time interval from the onset of the last cerebrovascular symptoms to the examinations of greater than 1 month; (5) DSA and ^{15}O gas PET conducted within an interval of 3 months in the chronic phase. Patients with subcortical cerebral infarcts measuring more than 3 cm in diameter or cortical cerebral infarcts in the ipsilateral MCA area or in the contralateral cerebral hemisphere (on MRI images), a history of intracerebral hemorrhage, head surgery, transient ischemic attacks or stroke in the hemisphere contralateral to arterial disease, clinical symptoms of ischemia in the vertebrobasilar artery territory or infarcts in the cerebellum or brainstem on MRI were excluded from the study. In addition, patients with the following disorders were also excluded: autoimmune disease, meningitis, brain neoplasm, Down's syndrome, Recklinghausen's disease, head trauma or irradiation to head. Six healthy persons (2 males and 4 females; mean age ± SD = 33 ± 6.6 years) were also enrolled in the study as normal controls. All of the control subjects had undergone ^{15}O gas PET. A detailed explanation of the purpose of the study and of all the procedures used in the study was given to all of the subjects prior to their enrollment. Written informed consent was obtained from each of the subjects. The study was approved by the Ethical Committee of Osaka University Hospital for Clinical Research.

Evaluation of DSA Images

The DSA images were first read independently by a neuroradiologist and a neurologist blinded to all clinical information about the subjects, and the decision about the presence of the moyamoya-like vascular abnormality was made by joint agreement at a conference between the two. Based on the presence or

Table 1. Symptoms, atherosclerotic lesions, vascularity and PET parameters in the ipsilateral hemispheres

Patient No.	Age years	Sex	Side	Symptoms	Site of lesion/ lesion type	Total vascularity index	PET parameters in the ipsilateral cortical MCA area			
							CBF ml/min/100 g	$CMRO_2$ ml/min/100 g	OEF %	CBV ml/100 g
Moyamoya syndrome group										
1	64	M	rt	TIA	rt MCA/O	8	39.5	2.90	51.1	6.92
2	65	F	rt	CI	rt MCA/O, rt PCA/S, bil ACA/O	5	31.1	2.52	56.9	4.14
3	74	F	rt	TIA	rt MCA/O, rt PCA/S	4	42.6	2.77	50.6	6.02
4	74	M	lt	CI	lt MCA/S	6	21.4	2.44	53.7	5.31
5	61	M	lt	TIA	lt MCA/S, bil ACA/S	6	23.2	2.46	53.6	4.75
6	63	M	rt	TIA, CI	rt ICA/O, rt PCA/S	7	26.3	2.52	55.8	5.08
7	69	F	rt	CI	rt MCA/S, bil ACA/S	4	33.8	3.66	59.5	5.76
Non-moyamoya-syndrome group										
8	57	F	rt	TIA	rt ICA/O	8	34.9	2.48	45.6	3.92
9	61	F	lt	TIA	lt ICA/O	8	48.3	2.62	36.5	4.38
10	55	M	lt	TIA	lt MCA/S, lt VA/S	6	36.4	2.99	45.1	4.01
11	58	M	rt	none	rt MCAO, lt VA/S	8	24.3	2.11	50.5	3.57
12	65	F	lt	TIA	lt MCA/O	8	33.5	3.14	57.1	4.88
13	66	M	lt	none	lt MCA/O	8	27.4	2.64	47.7	4.15
14	62	M	lt	none	lt MCA/O	8	27.2	2.13	46.5	4.32
15	62	M	lt	TIA	lt MCA/O	5	33.8	2.69	41.6	4.54
16	63	F	rt	none	rt MCA/S	7	38.7	2.73	43.6	4.45
17	39	M	rt	TIA	rt MCA/O	7	50.7	4.00	42.2	5.44
18	58	M	rt	CI	rt ICA/O	7	33.4	2.69	44.1	5.32
19	70	M	rt	TIA, CI	rt ICA/S	8	37.1	2.38	40.1	4.60
20	65	M	rt	TIA, CI	rt ICA/O	8	42.9	2.99	42.2	4.14
21	78	M	lt	TIA	lt ICA/S	7	32.9	2.65	52.8	4.16

rt = Right; lt = left; bil = bilateral; TIA = transient ischemic attack; CI = cerebral infarction; ICA = internal carotid artery; ACA = anterior cerebral artery; PCA = posterior cerebral artery; VA = vertebral artery; CBF = cerebral blood flow; $CMRO_2$ = cerebral metabolic rate of oxygen; OEF = oxygen extraction fraction; CBV = cerebral blood volume; S = stenosis; O = occlusion.

absence of the basal moyamoya-like vessels, the patients were classified into 2 groups: the moyamoya syndrome group (n = 7; 4 males and 3 females; mean age ± SD = 67 ± 5.3 years) and the non-moyamoya-syndrome group (n = 14; 10 males and 4 females; mean age ± SD = 65 ± 11 years). Figure 1a, b shows representative DSA images from the 2 groups. In all groups of patients, no apparent moyamoya-like vessels were found in any region other than the basal area. The interobserver agreement for this grouping was reasonably good ($\kappa = 0.8$). The clinical features of the patients in each group are shown in table 1.

In addition, the degree of regional or total vascularity in the ipsilateral cerebral hemisphere, excluding that of the basal moyamoya-like vessels, was evaluated in each patient by angiography. We applied a scoring system to access the patency of the ipsilateral MCA and to evaluate the degree of development of the leptomeningeal collateral circulation from the ipsilateral anterior cerebral arteries (ACA) or posterior cerebral arteries (PCA). Vascular patency of the MCA was classified into 4 grades (MCA vascularity index): grade 0, occlusion of the MCA with almost no visualization of the distal branches; grade 1, visualization of a single M2 branch; grade 2, visualization of more than two M2 branches; grade 3, normal MCA. The development of collateral vessels from the ACA was classified into 5 grades (ACA vascularity index): grade 0, occlusion of the ACA with almost no visual-

ization of the distal branches; grade 1, poor visualization of the distal branches of the ACA; grade 2, almost normal ACA with no development of leptomeningeal collateral vessels; grade 3, leptomeningeal cortical branches found in one lobe; grade 4, leptomeningeal cortical branches found in two or more lobes. Development of collateral vessels from the PCA was classified into 6 grades (PCA vascularity index): grade 0, occlusion of the PCA with almost no visualization of the distal branches; grade 1, poor visualization of the distal branches of the PCA; grade 2, almost normal PCA with no development of leptomeningeal collateral vessels; grade 3, leptomeningeal cortical branches found in one lobe; grade 4, leptomeningeal cortical branches found in two lobes; grade 5, leptomeningeal cortical branches found in more than three lobes. These vascularity indices were summed up in each patient as the total vascularity index in the ipsilateral hemisphere (maximum score: 12).

The extent of development of the basal moyamoya-like vessels was evaluated in anteroposterior-view DSA images in a plane perpendicular to the orbitomeatal (OM) line. The extension index of the basal moyamoya-like vessels was calculated as the distance from the root to the top-end of the basal moyamoya-like vessels divided by the distance from the base of the skull (top of the sella turcica) to the top of the skull in the same plane (fig. 1c).

PET Imaging

The Headtome V/SET 2400W system (Shimadzu, Kyoto, Japan) was used for the PET imaging. Prior to the emission scan, a Ge-68/Ga-68 transmission scan was performed for 10 min for attenuation correction. All scans were performed at a resolution of 3.7 mm full width at half maximum in the transaxial direction and of 5 mm full width at half maximum in the axial direction. Images were reconstructed using an ordered subset expectation maximization algorithm (12 iterations with 4 ordered subsets). Each subject's head was fixed in place with a head holder and positioned using light beams to obtain transaxial slices parallel to the orbitomeatal line. Data were formatted as a 3D dataset with 63 slices (3.17 mm thick) in 128 × 128 matrices. The cerebral blood flow (CBF), cerebral metabolic rate of oxygen ($CMRO_2$), oxygen extraction fraction (OEF) and cerebral blood volume (CBV) were measured using the conventional ^{15}O gas steady-state method [8]. The $CMRO_2$ and OEF were corrected by the CBV [9].

MRI

All the patients underwent PET and MRI within an interval of 3 months. Scans were obtained on the following scanners: GENESIS SIGNA 1.5T (GE Yokogawa Medical Systems, Tokyo, Japan), SIGNA EXCITE 1.5T (GE Healthcare, Chalfont St. Giles, UK), and MAGNETOM VISION 1.5T (Siemens, Erlangen, Germany). The MR protocol included T_2-weighted 2D fast spin echo sequences: (scan parameters: axial plane, FOV 250 mm, matrix 256 × 256 or 512 × 512, slice thickness: 5 mm, interslice gap 1–1.5 mm, TE: 90–131 ms, TR: 4,500–5,000 ms).

Data Analysis

Measurement of these parameters was executed in the ipsilateral MCA area using the automated constant region of interest (ROI) analysis software, FineSRT [10], which can perform the analysis using a precise constant 1,394 ROI (both hemispheres), with excellent objectivity and reproducibility. The MCA area was divided into 2 subdivisions: the cortical MCA area (i.e. the ipsilateral cortical MCA branch territory in the frontal, parietal and temporal lobes) and the basal ganglia, except the caudate nucleus. Ipsilateral ROI included in each of the two MCA divisions were selected from the constant 1,394 ROI and averaged. Statistical ROI analysis was carried out in each of the two subdivisions of the MCA area. Differences in the mean values among the groups were analyzed using a one-way ANOVA followed by the least significant difference test for ROI analysis, and the Mann-Whitney U test for other comparisons. Correlational analysis was performed by determining Spearman's rank-order correlation coefficient. Multivariate analysis was carried out by multiple linear regression analysis. Statistical significance was defined by a p value of less than 0.05.

Results

There were no significant differences in the clinical characteristics (age, gender, handedness, history of hypertension, hyperlipidemia and/or diabetes mellitus) or physiological parameters measured on the day of the PET study (blood pressure, partial pressure of arterial CO_2 and O_2, arterial pH, arterial O_2 saturation, hemoglobin and hematocrit) between the moyamoya syndrome group and the non-moyamoya-syndrome group. In the 17 symptomatic patients, there was no significant difference in the interval from the initial clinical symptoms to the time of performance of the DSA between the moyamoya syndrome group (n = 7, 55 ± 36 months) and the non-moyamoya-syndrome group (n = 10, 35 ± 20 months). Figure 2 shows the CBF, $CMRO_2$, OEF, CBV and CBF/CBV in the ipsilateral MCA area as measured by PET. The CBF was significantly lower in the moyamoya syndrome group than in the non-moyamoya-syndrome group in the ipsilateral cortical MCA area, and lower in the moyamoya syndrome group than in the normal controls in the basal ganglia. There was no significant difference in the $CMRO_2$ between the moyamoya syndrome group and the non-moyamoya-syndrome group in the whole MCA area, whereas the $CMRO_2$ values in the whole MCA area were significantly decreased in both the patient groups as compared with the values in the normal controls. The OEF was significantly higher in the moyamoya syndrome group than in the non-moyamoya-syndrome group in the cortical MCA area, but not in the basal ganglia. However, no significant difference in the OEF was found in the whole MCA area between the non-moyamoya-syndrome group and the normal controls. Although intergroup differences in the CBV were not significant as evaluated by ANOVA, the CBV in the moyamoya syndrome group was significantly higher than in the non-moya-

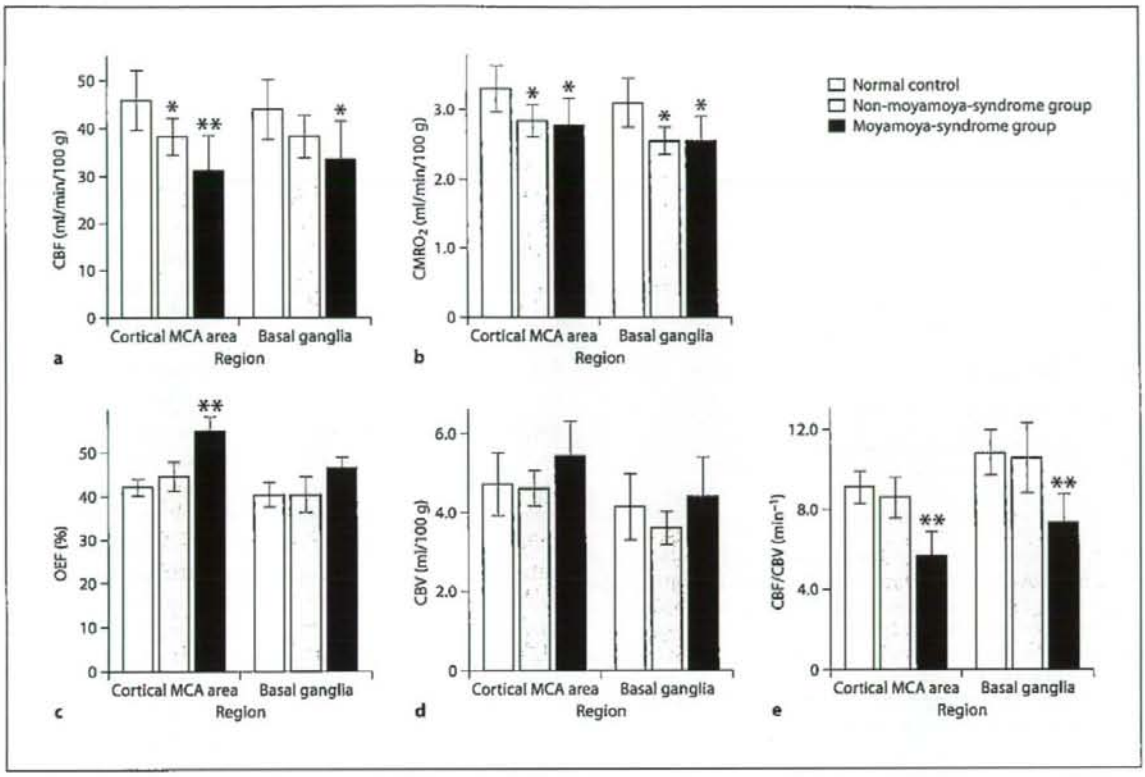

Fig. 2. Comparison of the regional CBF (**a**), regional $CMRO_2$ (**b**), regional OEF (**c**), regional CBV (**d**) and CBF divided by CBV (CBF/CBV; **e**) by the angiographic type. Data are shown as means plus 95% confidence intervals. Cortical MCA area = the ipsilateral cortical middle cerebral artery (MCA) branch territory in the frontal, parietal, and temporal lobes; basal ganglia = the ipsilateral basal nuclei except for the caudate nucleus. * $p < 0.05$ (one-way ANOVA followed by least significant difference test) versus normal control; ** $p < 0.05$ (ANOVA, least significant difference test) versus non-moyamoya-syndrome group and normal control.

moya-syndrome group in the cortical MCA area ($p = 0.03$) and the basal ganglia ($p = 0.04$), as determined by Mann-Whitney's U test. A significantly reduced CBF/CBV was found in the moyamoya syndrome group as compared with the non-moyamoya-syndrome group and normal controls in the whole MCA area. The atherosclerotic lesions in the ipsilateral hemisphere were more advanced in severity in the moyamoya syndrome group (table 1), and the total vascularity index was significantly lower in the moyamoya syndrome group than in the non-moyamoya-syndrome group ($p = 0.01$; table 1). Collateral flow from the external carotid artery to the ICA via retrograde flow through the ophthalmic artery was found only in patient No. 6. There was a weak negative correlation between the OEF in the cortical MCA area and the total vascularity index ($p = 0.06$). Multivariate linear regression analysis revealed that the OEF in the cortical MCA area remained significantly higher in the moyamoya syndrome group, even after controlling for the ACA, MCA and PCA vascularity indices ($p = 0.002$). In the moyamoya syndrome group, there was a significant correlation between the basal moyamoya-like vessel extension index and the OEF in the cortical MCA area ($r > 0.999$, $p < 0.001$; fig. 3); this correlation remained significant even after adjustment for the total vascularity index ($p = 0.02$).